Squeezing and expanding light without reflections via transformation optics

C. García-Meca,[1,*] M. M. Tung,[2] J. V. Galán,[1] R. Ortuño,[1] F. J. Rodríguez-Fortuño,[1] J. Martí,[1] and A. Martínez[1]

[1]*Valencia Nanophotonics Technology Center, Universidad Politécnica de Valencia, 46022 Valencia, Spain*
[2]*Instituto de Matemática Multidisciplinar, Universidad Politécnica de Valencia, 46022 Valencia, Spain*
**cargarm2@ntc.upv.es*

Abstract: We study the reflection properties of squeezing devices based on transformation optics. An analytical expression for the angle-dependent reflection coefficient of a generic three-dimensional squeezer is derived. In contrast with previous studies, we find that there exist several conditions that guarantee no reflections so it is possible to build transformation-optics-based reflectionless squeezers. Moreover, it is shown that the design of antireflective coatings for the non-reflectionless case can be reduced to matching the impedance between two dielectrics. We illustrate the potential of these devices by proposing two applications in which a reflectionless squeezer is the key element: an ultra-short perfect coupler for high-index nanophotonic waveguides and a completely flat reflectionless hyperlens. We also apply our theory to the coupling of two metallic waveguides with different cross-section. Finally, we show how the studied devices can be implemented with non-magnetic isotropic materials by using a quasi-conformal mapping technique.

OCIS codes: (160.3918) Metamaterials; (220.3630) Lenses; (230.0230) Optical devices.

References and links

1. R. Yang, M. A. Abushagur, and Z. Lu, "Efficiently squeezing near infrared light into a 21 nm-by-24 nm nanospot," Opt. Express **16**(24), 20142–20148 (2008).
2. L. Vivien, S. Laval, E. Cassan, X. Le Roux, and D. Pascal, "2-D taper for low-loss coupling between polarization-insensitive microwaveguides and single-mode optical fibers," J. Lightwave Technol. **21**(10), 2429–2433 (2003).
3. J. B. Pendry, D. Schurig, and D. R. Smith, "Controlling electromagnetic fields," Science **312**(5781), 1780–1782 (2006).
4. U. Leonhardt, and T. G. Philbin, "General Relativity in Electrical Engineering," N. J. Phys. **8**(10), 247 (2006).
5. M. Rahm, S. A. Cummer, D. Schurig, J. B. Pendry, and D. R. Smith, "Optical design of reflectionless complex media by finite embedded coordinate transformations," Phys. Rev. Lett. **100**(6), 063903 (2008).
6. M. Rahm, D. A. Roberts, J. B. Pendry, and D. R. Smith, "Transformation-optical design of adaptive beam bends and beam expanders," Opt. Express **16**(15), 11555–11567 (2008).
7. W. Yan, M. Yan, and M. Qiu, "Necessary and sufficient conditions for reflectionless transformation media in an isotropic and homogenous background," *arXiv:0806.3231v1* (2008).
8. T. M. Grzegorczyk, X. Chen, J. Pacheco, J. Chen, B. I. Wu, and J. A. Kong, "Reflection coefficients and Goos-Hanchen shifts in anisotropic and bianisotropic left-handed metamaterials," Prog. Electromagn. Res. **51**, 83–113 (2005).
9. E. Hecht, Optics, (Addison Wesley, 4th edition, 2001).
10. D. Taillaert, W. Bogaerts, P. Bienstman, T. F. Krauss, P. Van Daele, I. Moerman, S. Verstuyft, K. De Mesel, and R. Baets, "An out-of-plane grating coupler for efficient butt-coupling between compact planar waveguides and single-mode fibers," IEEE J. Quantum Electron. **38**(7), 949–955 (2002).
11. G. Roelkens, D. Vermeulen, D. Van Thourhout, R. Baets, S. Brision, P. Lyan, P. Gautier, and J. M. Fedeli, "High efficiency diffractive grating couplers for interfacing a single mode optical fiber with a nanophotonic silicon-on-insulator waveguide circuit," Appl. Phys. Lett. **92**(13), 131101 (2008).
12. T. Tsuchizawa, K. Yamada, H. Fukuda, T. Watanabe, J. Takahashi, M. Takahashi, T. Shoji, E. Tamechika, S. Itabashi, and H. Morita, "Microphotonics devices based on silicon microfabrication technology," IEEE J. Sel. Top. Quantum Electron. **11**(1), 232–240 (2005).
13. J. Li, and J. B. Pendry, "Hiding under the carpet: a new strategy for cloaking," Phys. Rev. Lett. **101**(20), 203901 (2008).

#136644 - $15.00 USD Received 26 Oct 2010; revised 30 Dec 2010; accepted 3 Jan 2011; published 9 Feb 2011

14. B. Vasić, G. Isic, R. Gajic, and K. Hingerl, "Coordinate transformation based design of confined metamaterial structures," Phys. Rev. B **79**(8), 85103 (2009).
15. V. M. Shalaev, "Physics. Transforming light," Science **322**(5900), 384–386 (2008).
16. Y. Xiong, Z. Liu, and X. Zhang, "A simple design of flat hyperlens for lithography and imaging with half-pitch resolution down to 20 nm," Appl. Phys. Lett. **94**(20), 203108 (2009).
17. A. V. Kildishev, and E. E. Narimanov, "Impedance-matched hyperlens," Opt. Lett. **32**(23), 3432–3434 (2007).
18. D. P. Gaillot, C. Croënne, F. Zhang, and D. Lippens, "Transformation optics for the full dielectric electromagnetic cloak and metal–dielectric planar hyperlens," N. J. Phys. **10**(11), 115039 (2008).
19. P. H. Tichit, S. N. Burokur, and A. de Lustrac, "Waveguide taper engineering using coordinate transformation technology," Opt. Express **18**(2), 767–772 (2010).
20. X. Zang, and C. Jiang, "Manipulating the field distribution via optical transformation," Opt. Express **18**(10), 10168–10176 (2010).
21. Z. Chang, X. Zhou, J. Hu, and G. Hu, "Design method for quasi-isotropic transformation materials based on inverse Laplace's equation with sliding boundaries," Opt. Express **18**(6), 6089–6096 (2010).

1. Introduction

The ability to squeeze and expand light has many applications in optics, ranging from beam collimation to nanolithography, optical data storage, imaging quality enhancing and efficient coupling to nanoscale structures [1,2]. Transformation optics offers a new way to achieve these effects, since it provides the necessary medium to force electromagnetic fields to undergo the spatial distortion introduced by a certain coordinate transformation [3,4]. Finite embedded coordinate transformations enables us to transfer light alterations, such as bends or shifts, from the transformed media to another one [5], so it appears that this technique is very adequate for building squeezing devices. A simple two-dimensional (2D) version of a compressing device embedded in free space was studied in [6], showing that unavoidable reflections appear in that case. Reflections imply power loss, which invalidates the utility of squeezers in many situations. The need for antireflective coatings was also observed in [6], although it was not clear at all how to design an antireflective coating for such a complex material and no hint was given in that study. Moreover, the conclusions drawn from the 2D case cannot be generalized to the three-dimensional (3D) one, as there can be fundamental differences between them. In addition, the heuristic condition for no reflections given in [6] only allows us to know whether the device is reflectionless for all angles or not. However, the reflected power depends on the polarization and on the angle, and could be negligible for certain spatial directions. Finally, in some situations it would be desirable that the output medium was different from the input one (in fact, we will take advantage of the squeezer properties in this situation to make a reflectionless device). Therefore, the possibility of achieving reflectionless squeezers is still open and a general study with the aim of obtaining this feature, indispensable for most applications, is lacking.

In this work, we develop a method to derive an analytical expression for the angle-dependent reflection coefficient of a generic 3D squeezer based on transformation optics, from which all the necessary information can be obtained. In contrast with previous studies, it is shown that squeezing devices based on transformation optics are reflectionless under certain conditions. In addition, we show that designing antireflective coatings for the non-reflectionless case can be reduced to matching the impedance between two dielectrics. Many applications could benefit from these devices. As an example, we show that they can implement completely flat reflectionless hyperlenses and ultra-short perfect spot-size converters (SSC) that couple light to high-index nanophotonic waveguides. Moreover, we use our theory to suppress the reflections appearing when transformation media are used to couple metallic waveguides with different cross-section. Finally, we propose a non-magnetic isotropic implementation of the studied squeezers (expanders) based on a quasi-conformal mapping technique.

2. Theory

In an isotropic homogeneous background, only rotations and displacements of the outer boundaries achieve all-angle reflectionless transformation media [7]. Thus, to build an all-angle reflectionless squeezer, which has a compressed boundary, it is necessary to consider a

#136644 - $15.00 USD Received 26 Oct 2010; revised 30 Dec 2010; accepted 3 Jan 2011; published 9 Feb 2011

more general scenario. Specifically, we will allow the medium that will be transformed into the squeezer to be different from the output medium in original space. This step is the key for some of the results obtained below. It is also important to consider a full problem with the possibility of a 3D transformation as mentioned above. Finally, our aim is to obtain an analytical expression for the total reflection coefficient of the squeezer, so that we can evaluate the reflected power and see if there is any preferred spatial direction for which no reflections occur. The problem under consideration is sketched in Fig. 1.

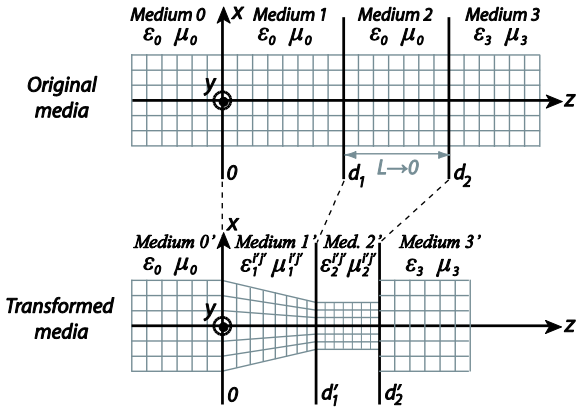

Fig. 1. Sketch of the problem. Cartesian coordinate mesh in the original media is "seen" distorted by the fields in the transformed media.

We start from Euclidean flat space with Cartesian coordinates denoted by x_i ($i=1,2,3$, $x_1=x$, $x_2=y$ and $x_3=z$) and map it to another space with coordinates x_i'. Both coordinate sets are related by $x_i'=f_i(x_j)$. We assume that in original space all media are isotropic. A pair of constitutive parameters $\varepsilon=\varepsilon_0\varepsilon_r$ and $\mu=\mu_0\mu_r$ in this space, becomes $\varepsilon^{i'j'}=(\epsilon^{klm}\Lambda_k^1\Lambda_l^2\Lambda_m^3)^{-1}g^{i'j'}\varepsilon$ and $\mu^{i'j'}=(\epsilon^{klm}\Lambda_k^1\Lambda_l^2\Lambda_m^3)^{-1}g^{i'j'}\mu$ in transformed space, where ϵ^{klm} and $\Lambda_i^{i'}$ are the Levi-Civita and Jacobian tensors, and $g^{i'j'}$ is the metric tensor in the transformed space [4]. In the materials interpretation [3,4], these are the media to be placed in physical space, represented by the original coordinate system, to modify the fields according to the transformations given by f_i. We have divided the problem into four slab-shaped regions (see Fig. 1). Medium 0 is air, from which light impinges onto medium 1. Mediums 1 and 2 are also air. Medium 3 (output medium), is isotropic and is characterized by ε_3 and μ_3. These media are transformed into those denoted by primed numbers according to the piecewise functions given by Eq. (1):

$$f_i := \begin{cases} x_i, & -\infty < z \le 0 \\ \left\{ h_i \middle| h_{(i),(i)}(z=0)=1, h_{(i),(i)}(z=d_1)=F_i \right\}, & 0 < z \le d_1 \\ x_k D_i^k, & d_1 < z \le d_2 \\ x_i-(d_2-d_2')\delta_{i1}, & d_2 < z < \infty \end{cases}, \qquad (1)$$

where $d_2'=d_2/F_3$ and we have defined $D_i^k=diag\left(1/F_1,1/F_2,1/F_3\right)$. No summation is to be performed over repeated indices in parentheses. Note the discontinuity in the transformation at $z=d_2$, which is in general the reason for reflections in embedded compressors. The transformation performed on media 0 and 3 does not change their parameters. Medium 1' (transformed medium 1) is the squeezer/expander. A continuous compression is made in it,

#136644 - $15.00 USD Received 26 Oct 2010; revised 30 Dec 2010; accepted 3 Jan 2011; published 9 Feb 2011

going from no compression at $z=0$ to a compression F_i in coordinate x_i at $z=d_1$ ($0<F_i<1$ means expansion). The parameters of medium 1', $\varepsilon_1^{i'j'}$ and $\mu_1^{i'j'}$, are inhomogeneous and generally quite complicated at $z=d_1$, making it very difficult to calculate the reflection between this medium and the output one. Our approach to calculate the squeezer's reflection is to introduce an auxiliary layer (medium 2 and its transformed counterpart medium 2'), in which the squeezer's compression at $z=d_1$ is kept constant. Thus, the relative constitutive parameters of medium 2' are:

$$\xi^{i'j'} := \varepsilon_{2r}^{i'j'} = \mu_{2r}^{i'j'} = F_1F_2F_3 diag(1/F_1^2, 1/F_2^2, 1/F_3^2). \quad (2)$$

Restricting ourselves to continuous transformations at the boundaries between media 0-1 and 1-2 ensures that no reflections will take place at these interfaces. The fact that $\xi^{i'j'}$ is homogeneous and has its principal components along the Cartesian axes greatly simplifies the problem of calculating the reflection coefficient R between media 2' and 3'. This can be done by matching the tangential components of the eigenmodes of an anisotropic homogeneous slab (medium 2') and the isotropic outer medium (medium 3′) at their interface [8]. R does not depend on the length L of medium 2. This enables us to make L tend to zero, so in practice this layer will not exist. We now analyze the case corresponding to $k_y=0$ (the derived formula can be generalized with some extra work), for which it can be shown that (see Appendix A):

$$R = \alpha \frac{\rho_3\sqrt{\omega^2\varepsilon_0\mu_0F_1^2 - k_x^2} - F_2\sqrt{\omega^2\varepsilon_3\mu_3 - k_x^2}}{\rho_3\sqrt{\omega^2\varepsilon_0\mu_0F_1^2 - k_x^2} + F_2\sqrt{\omega^2\varepsilon_3\mu_3 - k_x^2}}, \quad (3)$$

where $\rho_3=\varepsilon_{r3}$, $\alpha=-1$ for TM polarization (H field along y axis) and $\rho_3=\mu_{r3}$, $\alpha=1$ for TE polarization (E field along y axis). The cross-reflection coefficients between both polarizations are zero. Since reflection is only possible at this boundary, Eq. (3) expresses the total reflection of the squeezer/expander. First, we observe that R is independent of z compressions. Moreover, we can identify three very interesting cases in which reflection vanishes:

1. $\mu_{r3}=F_2=1$ and $\varepsilon_{r3}=F_1^2$ for TE incidence
2. $\mu_{r3}=1$ and $\varepsilon_{r3}=F_2=F_1^2$ for TM incidence
3. $\varepsilon_{r3}=\mu_{r3}=1$ and $F_1=F_2$ for normal incidence ($k_x=0$) and arbitrary polarization.

We have focused on non-magnetic output media, which are the most common ones. The first two cases tell us that $R=0$ if the outer medium is a certain dielectric. Note that allowing media 2 and 3 to be different has been crucial to find these two conditions. Remarkably, the third case indicates that, for normal incidence (which is the case in many applications), $R=0$ if we perform a uniform transversal compression from air to air. It has to be stressed that this condition cannot be found by studying a 2D problem. Going a step further, we would like to transfer squeezed light to any dielectric medium characterized by ε_d, regardless of the compression. The conditions for $R=0$ give us a key knowledge to achieve this. Since there are no reflections if the output dielectric permittivity is ε_3, we only need to match this dielectric to the desired one, with constant ε_d. Antireflective coatings engineering between two isotropic dielectrics is a much explored field that offers many simple and flexible options [9]. Therefore, a straight solution is to put the proper antireflective coating between the squeezer and the medium characterized by ε_d. This way the squeezer will be matched to ε_d

#136644 - $15.00 USD Received 26 Oct 2010; revised 30 Dec 2010; accepted 3 Jan 2011; published 9 Feb 2011

instead of ε_3 (no medium with ε_3 is then needed, as it happened with the auxiliary layer). Usually, antireflective coatings consist of one or few dielectric layers, depending on bandwidth and angular requirements. Placing a dielectric layer at the device's output is easier than implementing the squeezer and it does not pose a technological drawback. To verify our theoretical results, numerical simulations have been performed using COMSOL Multiphysics. As an example, we designed a 2D squeezer for *TE* polarization with $h_1 = x/(1+Cz)$, $h_2 = y$, $h_3 = z$, $C = (F_1 - 1)/d_1$ and $F_1 = 4$. Figure 2 shows its performance when the incident wave is a Gaussian beam.

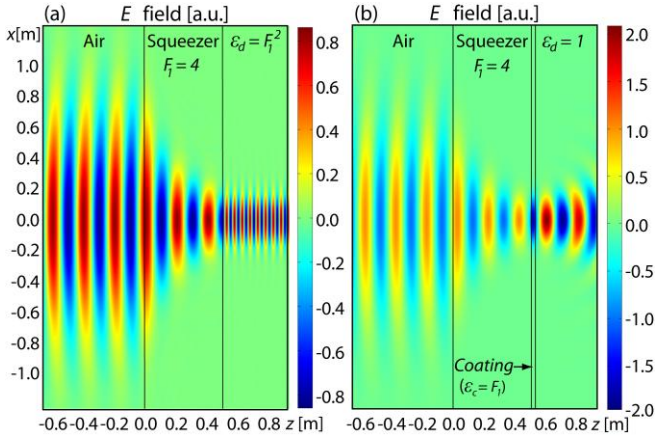

Fig. 2. Electric field distribution in the squeezer. The working wavelength is $\lambda = 0.2$ m. The relative permittivity of medium 3 is (a) $\varepsilon_{rd} = F_1^2$. (b) $\varepsilon_{rd} = 1$.

Two cases are considered. In the first one, the output medium is $\varepsilon_{rd} = \varepsilon_{r3} = F_1^2$ so that no antireflective coating is needed. In the second case, $\varepsilon_{rd} = 1$ and we use a $\lambda/4$ dielectric coating with constant ε_{rc}. It is known that if $\varepsilon_{rc}^2 = \varepsilon_{r3}\varepsilon_{rd}$, reflections are suppressed. In both cases, the calculated relative transmitted power $P_t = P_{out}/P_{in}$ is 100% (P_{in} and P_{out} are the squeezer input and output power). Without the coating, $P_t = 63\%$. We can verify this result with Eq. (3), as $P_t = 1 - |R|^2$. Since incidence is almost normal, we can put $k_x = 0$. Substituting the problem data in Eq. (3) we obtain $P_t = 64\%$, in very good agreement with numerical results. Note that the different *E* field intensities in the input and output media are consistent with the conservation of total power flow. It is also worth mentioning that the squeezer provides a compressed version of the fields inside it. This compression is transferred to the outside world near the squeezer. However, once the electromagnetic wave has exited the squeezer, it is subject to the diffraction laws of the output medium. Thus, the Gaussian beam exiting the squeezer will diverge as it propagates. This is mainly observed in Fig. 2(b), as this divergence is faster in air than in the medium with n = 4.

3. Applications

Applications of the proposed reflectionless device are straightforward. Here, two additional potential applications are proposed. The first one is a perfect squeezer-based spot size converter for an efficient coupling between an optical fibre and a high-index nanophotonic waveguide or nanowire, which is one of the most challenging tasks in the field of silicon photonics, due to the large mismatch in mode size of nanowires (sub-wavelength transversal dimensions) and standard single mode fibres (SMF, 10 μm mode diameter). Many solutions have been proposed, following one of these approaches: lateral (in plane) or vertical (out of

#136644 - $15.00 USD Received 26 Oct 2010; revised 30 Dec 2010; accepted 3 Jan 2011; published 9 Feb 2011

plane) coupling. The latter requires out of plane diffraction, usually via grating couplers, whose achievable efficiency with conventional designs is lower than 40% [10]. To reach higher efficiencies, highly sophisticated designs are needed, extremely increasing fabrication difficulty [11]. Lateral coupling implies 2D SSC via waveguide inverse tapering down to tens of nanometers wide [2], so matching the high SMF mode size is very challenging with a single inverted tapering structure. Most actual realizable single stage structures are limited in mode size to approximately 3-4 μm. Efficient coupling to such mode diameters can be achieved by means of lensed or high-numerical-aperture fibres with 3-4 μm mode diameters. Usually, in these structures the required inverted taper is longer than 200 μm and maximum coupling efficiency is lower than 80% [12]. We aim to use our squeezer as an efficient SSC with a dramatically reduced length while achieving 100% coupling efficiency. Thus, the squeezer must compress incoming light fitting its size to that of the waveguide and then deliver the compressed beam to the waveguide without reflections, i.e., match air to the waveguide high-index core. Then, light is kept confined in the waveguide by total internal reflection (TIR) (see Fig. 3).

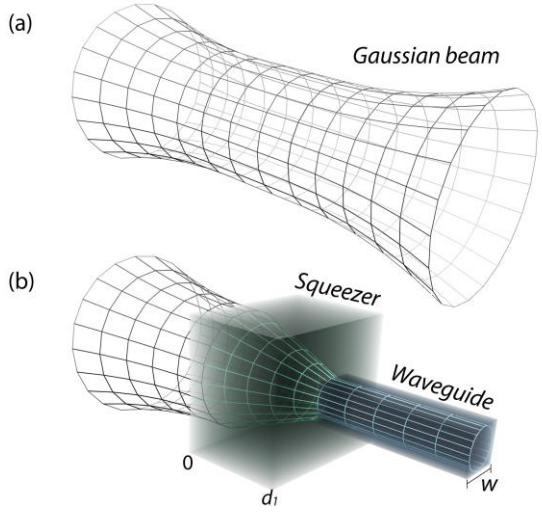

Fig. 3. (a) Gaussian beam propagating in free space. (b) The squeezer couples the beam to a nanophotonic dielectric waveguide.

We will assume the telecom wavelength $\lambda = 1.5\mu m$, and a waveguide with sub-wavelength width w = 1 μm and refractive index n = 4, as in the example of Fig. 2 (the problem would be very similar if we used silicon, since $n_{Si} = 3.45$ in this band).

We limit our study to a 2D case due to the computational complexity of the 3D problem. Given the size of the input beam, a compression $F_1 = 4$ is enough, which satisfies condition 1 for no reflections. A seamless coupling can be observed in Fig. 4(b).

#136644 - $15.00 USD Received 26 Oct 2010; revised 30 Dec 2010; accepted 3 Jan 2011; published 9 Feb 2011

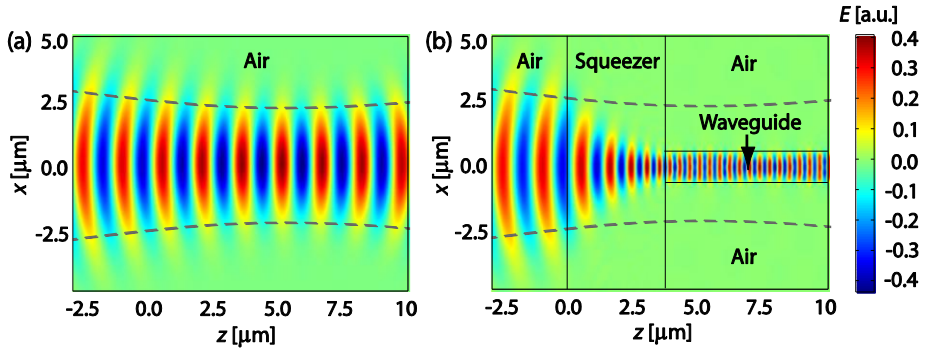

Fig. 4. (a) Simulation of a 2D Gaussian beam propagating in free space. (b) The beam in (a) is squeezed and perfectly coupled to the nanophotonic waveguide.

Numerical calculations reveal that $P_t = 100\%$ again, where P_{out} has been evaluated at the right waveguide end. Without the squeezer, $P_t < 40\%$ and decreases with z due to an inefficient mode matching. To extend the application to larger compression factors, antireflective coatings are necessary. In a 3D problem, compression in both transversal directions is demanded. Since in this application we have normal incidence, a squeezer fulfilling condition 3 with the proper antireflective coating can be employed. As for its size, the squeezer can be as short as desired. Nonetheless, the necessary constitutive parameters become extreme as we reduce d_1. A surprisingly small length below 10 μm, far below the current state of the art, is enough to achieve a set of parameters with very moderate values for the 2D and 3D cases. Although fabrication of the 3D squeezer would be challenging, it is worth pointing out that the quasi-conformal mapping technique introduced in [13] would provide a practically realizable non-magnetic isotropic implementation for the 2D squeezer, as we will see in section 4. Regardless of its application as SSC, our squeezer-TIR waveguide device presents the important advantage of using an isotropic homogeneous dielectric as the guiding element, as opposed to previously proposed squeezers based on transformation optics [14], where complex materials are needed.

The second application that we propose is a flat hyperlens that uses our reflectionless device as a wave expander. It is known that subwavelength spatial features of light sources are lost in the far field, since they are carried by evanescent waves that decay exponentially with distance. A hyperlens transforms evanescent components into propagating ones by magnifying the near field pattern, which can then be treated with conventional optics. Original hyperlenses had cylindrical geometry and suffered from reflections, two undesired features [15]. A flat hyperlens arising from the truncation of the original design was presented in [16], although the truncation gave rise to a variable gain, stronger at the hyperlens centre. Transformation optics has led to alternative designs that improved the impedance matching and made one of the two lens surfaces flat [15,17]. A hyperlens with both flat surfaces was proposed in [18]. However, it is not reflectionless and, as no expansion in z direction is made, its width must be extremely small. The above theoretical results, enables us to design an expander that implements a completely flat reflectionless hyperlens. Following a similar approach to that of [17], we transform a little slab of length d_1 into a larger slab of length d_1' (this can be done without affecting the reflection properties of the device, since the reflection coefficient is independent of compressions/expansions in z direction as was shown above), while expanding the fields in x direction at the same time. This transformation can be described by $h_1 = x/(1+C_1 z)$, $h_2 = y$, and $h_3 = z/(1+C_2 z)$, with $C_1 = (F_1 - 1)/d_1$, $C_2 = (F_3^{1/2} - 1)/d_1$ and $F_1, F_3 < 1$. Since light goes from air to air, antireflective coatings are needed. An interesting particular case is that in which the sources are embedded in a dielectric medium with constant $\varepsilon_{r3} = n_3^2$. In this case we can use a squeezer from air to that dielectric,

#136644 - $15.00 USD Received 26 Oct 2010; revised 30 Dec 2010; accepted 3 Jan 2011; published 9 Feb 2011

described by the previous functions with the same value of F_3 and satisfying $F_1 = n_3$ (no coating is needed in this case). Since light now travels from right to left (according to Fig. 1), the squeezer acts as an expander. Propagating components inside the dielectric also become propagating in air, improving the resolution by F_1, in a similar way to solid immersion lenses, with the advantage of being flat and reflectionless. Note that this lens can perform in far field. In Fig. 5 we provide a numerical example with $F_1 = 2$, $F_3 = 1/100$ and $d_1 = \lambda/20$, where two test point sources separated by $\lambda/4$ are placed near the lens left surface (for better clarity, in Fig. 5 the squeezing device is flipped from left to right as compared to the previous figures). The magnitude of the resulting power flow is shown in Fig. 5. Cuts at $z = 0$ (the lens output) and at a distance $\lambda/20$ away from the sources without the lens are also depicted. Clearly, the device provides a magnified image of the fields where the images of the two sources are separated by $\lambda/2$.

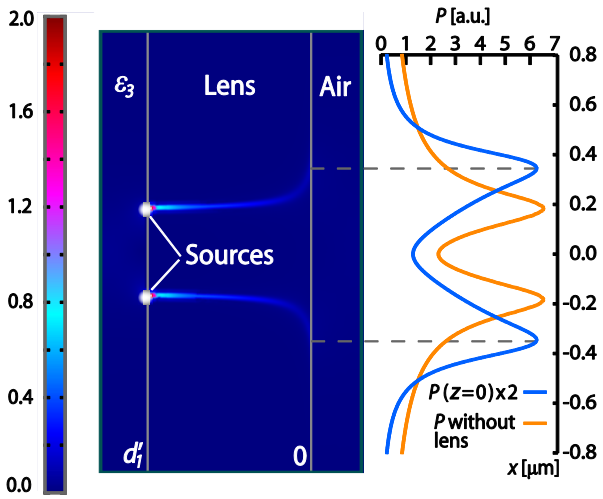

Fig. 5. Lens power flow distribution. The working wavelength is $\lambda = 1.5$ μm.

Finally, we apply our theoretical results to the coupling between two metallic waveguides of different transverse size. Several devices based on transformation optics have been proposed to solve this problem [19,20]. However, as in the other cases, the problem of reflections has not been addressed. In these works, some simple compressing or expanding spatial transformation is applied to adapt the dimensions of one waveguide to the other one. This way, and according to our previous theoretical results, a mismatch between the modes supported by the coupler and the outer medium (in this case, the output waveguide) is introduced. As an example, let us assume that we desire to couple a waveguide W1 of transverse size *a*, to another waveguide W2 of transverse size *a*/2, where we only excite the first TE mode at the left end of waveguide W1. In Fig. 6, we show the norm of the electric field for different solutions to this problem. In Fig. 6(a), no coupler is used and we just linearly change the metallic boundary of the waveguide. The strong modulation appearing in waveguide W1 and the transition waveguide indicates that high reflections are taking place at the boundary between the transition waveguide and waveguide W2.

In Fig. 6(b), we use a coupler that implements a linear spatial transformation from a transverse size of *a*, to a transverse size of *a*/2 ($F_1 = 2$), similar to the one employed in the previous examples and to those in [19,20]. Again, strong reflections are observed.

#136644 - $15.00 USD Received 26 Oct 2010; revised 30 Dec 2010; accepted 3 Jan 2011; published 9 Feb 2011

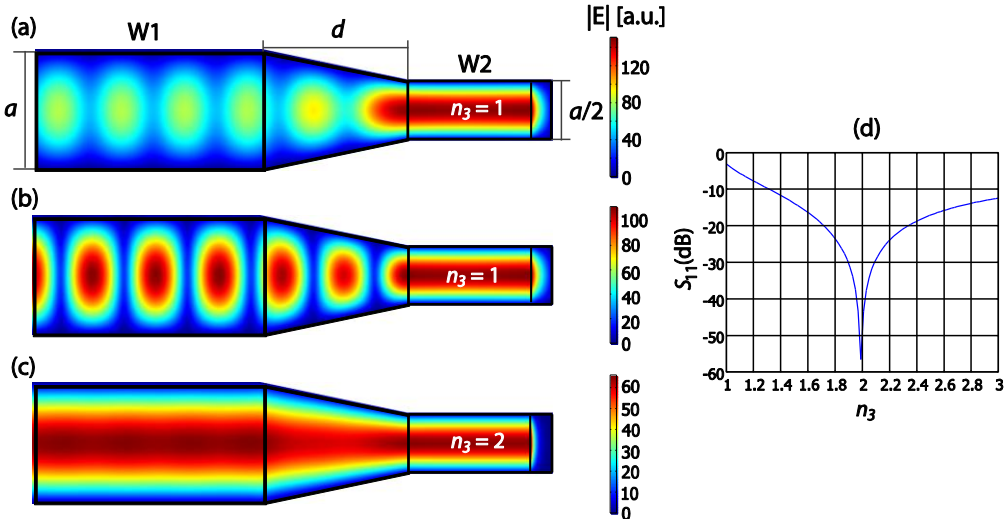

Fig. 6. Several solutions for coupling two metallic waveguides of different transverse size. In this example, a=0.4 m and d=0.5 m. The free space wavelength is $\lambda = 0.37$ m, below cut-off in all waveguides. |E| distribution (a) without coupler, (b) with coupler and n_3 = 1, and (c) with coupler and n_3=2. (d) S_{11} parameter as a function of n_3 when the coupler is used.

Now we apply our theory to this example. To a first approximation, we assume that the effective indices in waveguides W1 and W2 are those of the filling medium. Therefore, in Fig. 6(b), $\varepsilon_{r3} = n_3^2 = 1$. Obviously, reflections appear because we are not fulfilling condition 1. This can be easily solved by filling waveguide W2 with a material $n_3 = 2$ [Fig. 6(c)]. In this case, no modulation of the electric field is observed, showing that reflections have been suppressed. Alternatively, if we want waveguide W2 to be empty, we can design and use a dielectric antireflective coating following the procedure described above. This way, a perfect coupling between both waveguides is achieved. In Fig. 6(d), we depict the scattering parameter S_{11} as a function of the refractive index of the filling medium of waveguide W2, for the case where the coupler is used [as in Figs. 6(b) and 6(c)]. A pronounced minimum is clearly seen very close to $n_3 = 2$, validating our choice of effective indices.

4. Practical implementation

Although the main goal of this work is to study the reflections between squeezers (expanders) based on non-continuous transformations, we are also concerned with the practical implementation of these devices. In general, transformation media require anisotropic materials difficult to fabricate in practice. For instance, the specific implementations proposed in [19,20] would challenge current state of the art fabrication capabilities. Another disadvantage is that lossy resonant elements would be necessary. In the previous section, we mentioned that it would be possible to use a special mapping technique known as quasi-conformal mapping to achieve a non-magnetic isotropic realization for the 2D squeezers [13]. By using this technique anisotropy is minimized in such a way that the in-plane components of the constitutive tensors approach unity. We can neglect this slight anisotropy and implement the squeezer by using only a certain refractive index distribution. To this end, we follow the procedure described in [21] to transform a piece of waveguide W1 into the squeezer. In Fig. 7(a) we show the norm of the electric field for this case. All parameters are the same as in Fig. 6(c), except for the fact that the squeezer is made up of an isotropic non-magnetic material, i.e., just a spatially varying refractive index.

#136644 - $15.00 USD Received 26 Oct 2010; revised 30 Dec 2010; accepted 3 Jan 2011; published 9 Feb 2011

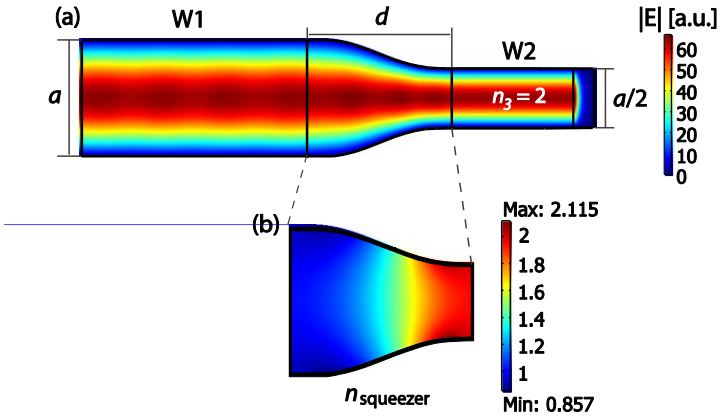

Fig. 7. Implementation of the squeezer with an isotropic spatially varying refractive index. (a) |E| field distribution. (b) Refractive index profile of the squeezer. For this particular implementation we obtained an anisotropy factor, as defined in [13], of 1.025. We employed a smooth cosine-like profile for the squeezer.

We can see in Fig. 7 that there are almost no reflections in this case either. Specifically, we obtained from the simulation a reflected power of 0.0036%. Thus, we have shown that it is possible to couple both waveguides with only a certain refractive index distribution. In this specific implementation, the required refractive index varies between 0.86 and 2.1 [see Fig. 7(b)]. Although it is possible to implement a refractive index below unity, it is preferable to have a refractive index range higher or equal to unity. For that purpose, we can just approximate the index by unity in the small regions where it is lower than one. Another possibility is to divide the whole index distribution by its minimum value (0.86). This does not affect the functionality of the device and introduces very weak reflections (as shown by numerical calculations) because the index mismatch is very low. We can of course completely avoid reflections by using the appropriate anti-reflective coating.

5. Conclusion

In summary, we have derived an analytical expression for the reflection coefficient of an optically transformed embedded squeezer. We have found the conditions for no reflections, showing how antireflective coatings can be used in non-reflectionless cases. This study has allowed us to design an ultra-short perfect SSC, as well as a completely flat reflectionless hyperlens. In addition, we have shown how to eliminate the reflections that appear when transformation optics-based devices are used to couple metallic waveguides with different cross-section. Finally, we have proposed a non-magnetic isotropic implementation of the constructed 2D squeezers/expanders, which only requires a spatially varying refractive index distribution.

Appendix A. Derivation of the reflection and transmission coefficients

In this section we derive Eq. (3). We start from macroscopic Maxwell's equations (assuming that the time dependence of the fields is of the form $e^{-i\omega t}$):

$$\begin{aligned} \nabla \times E &= i\omega B \\ \nabla \times H &= -i\omega B \end{aligned} \tag{A.1}$$

Together with the constitutive relations:

$$\begin{aligned} D &= \varepsilon . E \\ B &= \mu . H \end{aligned} \tag{A.2}$$

with:

#136644 - $15.00 USD Received 26 Oct 2010; revised 30 Dec 2010; accepted 3 Jan 2011; published 9 Feb 2011

$$\varepsilon = \begin{pmatrix} \varepsilon_{11} & \varepsilon_{12} & \varepsilon_{13} \\ \varepsilon_{21} & \varepsilon_{22} & \varepsilon_{23} \\ \varepsilon_{31} & \varepsilon_{32} & \varepsilon_{33} \end{pmatrix} \quad \mu = \begin{pmatrix} \mu_{11} & \mu_{12} & \mu_{13} \\ \mu_{21} & \mu_{22} & \mu_{23} \\ \mu_{31} & \mu_{32} & \mu_{33} \end{pmatrix} \tag{A.3}$$

Now we define the tensors (analogous expressions are defined for μ_{tt}, μ_{tz} and μ_{zt}):

$$\varepsilon_{tt} = \begin{pmatrix} \varepsilon_{11} & \varepsilon_{12} & 0 \\ \varepsilon_{21} & \varepsilon_{22} & 0 \\ 0 & 0 & 0 \end{pmatrix} \quad \varepsilon_{tz} = \begin{pmatrix} 0 & 0 & \varepsilon_{13} \\ 0 & 0 & \varepsilon_{23} \\ 0 & 0 & 0 \end{pmatrix} \quad \varepsilon_{zt} = \begin{pmatrix} 0 & 0 & 0 \\ 0 & 0 & 0 \\ \varepsilon_{31} & \varepsilon_{32} & 0 \end{pmatrix} \tag{A.4}$$

and separate Maxwell's equations in their transverse and longitudinal components in Cartesian coordinates:

$$i\mathrm{k}_t \times E_z\hat{z} + \hat{z} \times \frac{\partial \mathrm{E}_t}{\partial \mathrm{z}} = i\omega\mu_{tt} \cdot \mathrm{H}_t + i\omega\mu_{tz} \cdot H_z\hat{z} \tag{A.5}$$

$$i\mathrm{k}_t \times \mathrm{E}_t = i\omega\mu_{zt} \cdot \mathrm{H}_t + i\omega\mu_{33}H_z\hat{z} \tag{A.6}$$

$$i\mathrm{k}_t \times H_z\hat{z} + \hat{z} \times \frac{\partial \mathrm{H}_t}{\partial \mathrm{z}} = -i\omega\varepsilon_{tt} \cdot \mathrm{E}_t - i\omega\varepsilon_{tz} \cdot E_z\hat{z} \tag{A.7}$$

$$i\mathrm{k}_t \times \mathrm{H}_t = -i\omega\varepsilon_{zt} \cdot \mathrm{E}_t - i\omega\varepsilon_{33}E_z\hat{z} \tag{A.8}$$

where $\mathrm{E}_t = E_x\hat{x} + E_y\hat{y}$, $\mathrm{H}_t = H_x\hat{x} + H_y\hat{y}$, $\mathrm{k}_t = k_x\hat{x} + k_y\hat{y}$ and we have assumed a spatial dependence of the fields of the form $e^{i\vec{k}\cdot\vec{r}}$. From Eqs. (A.6) and (A.8), the longitudinal components of the fields can be expressed as a function of the transverse ones:

$$H_z\hat{z} = \frac{1}{\omega\mu_{33}}\mathrm{k}_t \times \mathrm{E}_t - \frac{1}{\mu_{33}}\mu_{zt} \cdot \mathrm{H}_t \tag{A.9}$$

$$E_z\hat{z} = -\frac{1}{\omega\varepsilon_{33}}\mathrm{k}_t \times \mathrm{H}_t - \frac{1}{\varepsilon_{33}}\varepsilon_{zt} \cdot \mathrm{E}_t \tag{A.10}$$

Upon substitution of Eq. (A.5) and (A.7) in Eq. (A.9) and (A.10), we arrive to:

$$\begin{aligned} \frac{\partial \mathrm{E}_t}{\partial \mathrm{z}} = &\left(-\frac{i}{\mu_{33}}\hat{z} \times \mathrm{I} \cdot \mu_{tz} \cdot \mathrm{k}_t \times \mathrm{I} - \frac{i}{\varepsilon_{33}}\hat{z} \times \mathrm{I} \cdot \mathrm{k}_t \times \mathrm{I} \cdot \varepsilon_{zt} \right) \cdot \mathrm{E}_t + \\ &+ \left(-i\omega\hat{z} \times \mathrm{I} \cdot \mu_{tt} + \frac{i\omega}{\mu_{33}}\hat{z} \times \mathrm{I} \cdot \mu_{tz} \cdot \mu_{zt} - \frac{i}{\omega\varepsilon_{33}}\hat{z} \times \mathrm{I} \cdot \mathrm{k}_t \times \mathrm{I} \cdot \mathrm{k}_t \times \mathrm{I} \right) \cdot \mathrm{H}_t \end{aligned} \tag{A.11}$$

$$\begin{aligned} \frac{\partial \mathrm{H}_t}{\partial \mathrm{z}} = &\left(i\omega\hat{z} \times \mathrm{I} \cdot \varepsilon_{tt} - \frac{i\omega}{\varepsilon_{33}}\hat{z} \times \mathrm{I} \cdot \varepsilon_{tz} \cdot \varepsilon_{zt} + \frac{i}{\omega\mu_{33}}\hat{z} \times \mathrm{I} \cdot \mathrm{k}_t \times \mathrm{I} \cdot \mathrm{k}_t \times \mathrm{I} \right) \cdot \mathrm{E}_t + \\ &+ \left(-\frac{i}{\varepsilon_{33}}\hat{z} \times \mathrm{I} \cdot \varepsilon_{tz} \cdot \mathrm{k}_t \times \mathrm{I} - \frac{i}{\mu_{33}}\hat{z} \times \mathrm{I} \cdot \mathrm{k}_t \times \mathrm{I} \cdot \mu_{zt} \right) \cdot \mathrm{H}_t \end{aligned} \tag{A.12}$$

where $\mathrm{I} = \hat{x}\hat{x} + \hat{y}\hat{y} + \hat{z}\hat{z}$. As stated above, we will limit ourselves to $k_y = 0$. In addition, the problem is simplified due to the fact that both the auxiliary layer and the outer medium are characterized by diagonal constitutive parameters. Given these simplifications and considering that $\frac{\partial}{\partial z} = ik_z$, Eq. (A.11) and (A.12) reduce to:

#136644 - $15.00 USD Received 26 Oct 2010; revised 30 Dec 2010; accepted 3 Jan 2011; published 9 Feb 2011

$$ik_z\begin{pmatrix}\mathrm{E}_t\\ \mathrm{H}_t\end{pmatrix}=\mathrm{A}\cdot\begin{pmatrix}\mathrm{E}_t\\ \mathrm{H}_t\end{pmatrix} \tag{A.13}$$

$$\mathrm{A}=\begin{pmatrix}0 & 0 & 0 & -\dfrac{ik_x^2}{\varepsilon_{33}\omega}+i\omega\mu_{22}\\ 0 & 0 & -i\omega\mu_{11} & 0\\ 0 & \dfrac{ik_x^2}{\mu_{33}\omega}-i\omega\varepsilon_{22} & 0 & 0\\ i\omega\varepsilon_{11} & 0 & 0 & 0\end{pmatrix} \tag{A.14}$$

This is an eigenvalue problem with four solutions. From the eigenvalues ik_z we find the four possible values of k_z (two for TE polarization and two for TM polarization), together with their corresponding eigenvectors (polarization states):

$$\mathtt{TE}:\ k_z^{1,2}=\pm\sqrt{\frac{\mu_{11}}{\mu_{33}}\left(\omega^2\varepsilon_{22}\mu_{33}-k_x^2\right)}\qquad \mathrm{E}_t=E\hat{y}\quad \mathrm{H}_t=E\frac{k_Z^{1,2}}{\omega\mu_{11}}\hat{x} \tag{A.15}$$

$$\mathtt{TM}:\ k_z^{3,4}=\pm\sqrt{\frac{\varepsilon_{11}}{\varepsilon_{33}}\left(\omega^2\mu_{22}\varepsilon_{33}-k_x^2\right)}\qquad \mathrm{E}_t=E\hat{x}\quad \mathrm{H}_t=-E\frac{\omega\varepsilon_{11}}{k_Z^{3,4}}\hat{y} \tag{A.16}$$

Now we particularize Eq. (A.15) and (A.16) for the parameters of the auxiliary layer and the outer medium. The parameters of the former correspond to a transformation medium associated with the transformation $x_i'=x_{(i)}/F_{(i)}$, which leads to:

$$\begin{aligned}\varepsilon_2^{ij}&=\varepsilon_0\xi^{ij}\\ \mu_2^{ij}&=\mu_0\xi^{ij}\end{aligned} \tag{A.17}$$

$$\xi^{ij}=F_1F_2F_3\begin{pmatrix}\dfrac{1}{F_1} & 0 & 0\\ 0 & \dfrac{1}{F_2} & 0\\ 0 & 0 & \dfrac{1}{F_3}\end{pmatrix}^T\begin{pmatrix}\dfrac{1}{F_1} & 0 & 0\\ 0 & \dfrac{1}{F_2} & 0\\ 0 & 0 & \dfrac{1}{F_3}\end{pmatrix}=\begin{pmatrix}\dfrac{F_2F_3}{F_1} & 0 & 0\\ 0 & \dfrac{F_1F_3}{F_2} & 0\\ 0 & 0 & \dfrac{F_1F_2}{F_3}\end{pmatrix} \tag{A.18}$$

This agrees with Eq. (2). In the case of the isotropic outer medium, we have:

$$\begin{aligned}\varepsilon_3^{ij}&=\varepsilon_3\delta^{ij}\\ \mu_3^{ij}&=\mu_3\delta^{ij}\end{aligned} \tag{A.19}$$

Substituting Eqs. (A.17)–(A.19) into Eqs (A.15)–(A.16), we have:

$$\mathtt{TE}:\quad k_{z,aux}^{1,2}=\pm\sqrt{\frac{\xi_{11}}{\xi_{33}}\left(\omega^2\varepsilon_0\mu_0\xi_{22}\xi_{33}-k_x^2\right)}\quad \mathrm{E}_t=E\hat{y}\quad \mathrm{H}_t=E\frac{k_{z,aux}^{1,2}}{\omega\mu_0\xi_{11}}\hat{x} \tag{A.20}$$

$$\mathtt{TM}:\ k_{z,aux}^{3,4}=\pm\sqrt{\frac{\xi_{11}}{\xi_{33}}\left(\omega^2\varepsilon_0\mu_0\xi_{22}\xi_{33}-k_x^2\right)}\quad \mathrm{E}_t=E\hat{x}\quad \mathrm{H}_t=-E\frac{\omega\varepsilon_0\xi_{11}}{k_{z,aux}^{3,4}}\hat{y} \tag{A.21}$$

#136644 - $15.00 USD Received 26 Oct 2010; revised 30 Dec 2010; accepted 3 Jan 2011; published 9 Feb 2011

for the auxiliary layer, and:

$$\text{TE}: \quad k_{z,out}^{1,2} = \pm\sqrt{\omega^2\varepsilon_3\mu_3 - k_x^2} \qquad \mathrm{E}_t = E\hat{y} \quad \mathrm{H}_t = E\frac{k_{z,out}^{1,2}}{\omega\mu_3}\hat{x} \tag{A.22}$$

$$\text{TM}: \quad k_{z,out}^{3,4} = \pm\sqrt{\omega^2\varepsilon_3\mu_3 - k_x^2} \qquad \mathrm{E}_t = E\hat{x} \quad \mathrm{H}_t = -E\frac{\omega\varepsilon_3}{k_{z,out}^{3,4}}\hat{y} \tag{A.23}$$

for the outer medium. Finally, we obtain the reflection coefficients for both TE and TM excitation. To this end, we suppose and incident field (TE or TM) in the auxiliary layer propagating towards the outer medium and see if there are TE or TM reflected and transmitted waves, demanding equality of the tangential fields at the boundary between both media. For simplicity, we assume that z = 0 at the boundary. For TE excitation we have in matrix notation:

$$\begin{pmatrix} 0 \\ 1 \\ -\dfrac{k_{z,aux}^1}{\omega\mu_0\xi_{11}} \\ 0 \end{pmatrix} + R_{11}\begin{pmatrix} 0 \\ 1 \\ \dfrac{k_{z,aux}^1}{\omega\mu_0\xi_{11}} \\ 0 \end{pmatrix} + R_{21}\begin{pmatrix} 1 \\ 0 \\ 0 \\ -\dfrac{\omega\varepsilon_0\xi_{11}}{k_{z,aux}^1} \end{pmatrix} = T_{11}\begin{pmatrix} 0 \\ 1 \\ -\dfrac{k_{z,out}^1}{\omega\mu_3} \\ 0 \end{pmatrix} + T_{21}\begin{pmatrix} 1 \\ 0 \\ 0 \\ \dfrac{\omega\varepsilon}{k_{z,out}^1} \end{pmatrix} \tag{A.24}$$

from which we deduce that:

$$R_{21} = T_{21} = 0 \tag{A.25}$$

$$R_{11} = \frac{\mu_3 k_{z,aux}^1 - \mu_0\xi_{11}k_{z,out}^1}{\mu_3 k_{z,aux}^1 + \mu_0\xi_{11}k_{z,out}^1} \qquad T_{11} = \frac{2\mu_3 k_{z,aux}^1}{\mu_3 k_{z,aux}^1 + \mu_0\xi_{11}k_{z,out}^1} \tag{A.26}$$

R_{11} and T_{11} are the TE reflection and transmission coefficients for TE excitation. R_{21} and T_{21} are the cross-polarization reflection and transmission coefficients from TE excitation to TM polarized waves. Analogously, for the TM case we have:

$$\begin{pmatrix} 1 \\ 0 \\ 0 \\ \dfrac{\omega\varepsilon_0\xi_{11}}{k_{z,aux}^1} \end{pmatrix} + R_{12}\begin{pmatrix} 0 \\ 1 \\ \dfrac{k_{z,aux}^1}{\omega\mu_0\xi_{11}} \\ 0 \end{pmatrix} + R_{22}\begin{pmatrix} 1 \\ 0 \\ 0 \\ -\dfrac{\omega\varepsilon_0\xi_{11}}{k_{z,aux}^1} \end{pmatrix} = T_{12}\begin{pmatrix} 0 \\ 1 \\ -\dfrac{k_{z,out}^1}{\omega\mu_3} \\ 0 \end{pmatrix} + T_{22}\begin{pmatrix} 1 \\ 0 \\ 0 \\ \dfrac{\omega\varepsilon}{k_{z,out}^1} \end{pmatrix} \tag{A.27}$$

and:

$$R_{12} = T_{12} = 0 \tag{A.28}$$

$$R_{22} = \frac{\xi_{11}\varepsilon_0 k_{z,out}^1 - \varepsilon_3 k_{z,aux}^1}{\xi_{11}\varepsilon_0 k_{z,out}^1 + \varepsilon_3 k_{z,aux}^1} \qquad T_{22} = \frac{2\xi_{11}\varepsilon_0 k_{z,out}^1}{\xi_{11}\varepsilon_0 k_{z,out}^1 + \varepsilon_3 k_{z,aux}^1} \tag{A.29}$$

In a similar way to the previous case, R_{22} and T_{22} are the TM reflection and transmission coefficients for TM excitation. R_{12} and T_{12} are the cross-polarization reflection and transmission coefficients from TM excitation to TE polarized waves. Finally, substituting Eq. (A.18) and Eqs. (A.20)–(A.23) into the previous equations, we arrive to Eq. (3):

#136644 - $15.00 USD Received 26 Oct 2010; revised 30 Dec 2010; accepted 3 Jan 2011; published 9 Feb 2011

$$R_{TE} = R_{11} = \frac{\mu_{r3}\sqrt{\omega^2\varepsilon_0\mu_0 F_1^2 - k_x^2} - F_2\sqrt{\omega^2\varepsilon_3\mu_3 - k_x^2}}{\mu_{r3}\sqrt{\omega^2\varepsilon_0\mu_0 F_1^2 - k_x^2} + F_2\sqrt{\omega^2\varepsilon_3\mu_3 - k_x^2}} \quad \text{(A.30)}$$

$$R_{TM} = R_{22} = \frac{F_2\sqrt{\omega^2\varepsilon_3\mu_3 - k_x^2} - \varepsilon_{r3}\sqrt{\omega^2\varepsilon_0\mu_0 F_1^2 - k_x^2}}{F_2\sqrt{\omega^2\varepsilon_3\mu_3 - k_x^2} + \varepsilon_{r3}\sqrt{\omega^2\varepsilon_0\mu_0 F_1^2 - k_x^2}} \quad \text{(A.31)}$$

Acknowledgements

Financial support by the Spanish MICINN under contract CONSOLIDER EMET (CSD2008-00066) and PROMETEO-2010-087 R&D Excellency Program (NANOMET) is gratefully acknowledged. C. G.-M., R. O. and F.J. R.-F. acknowledge financial support from grants FPU of MICINN, FPI of U.P.V. and FPI of Generalitat Valenciana, respectively.